Performance of Bed-Load Transport Equations Relative to Geomorphic Significance: Predicting Effective Discharge and Its Transport Rate

Jeffrey J. Barry[1]; John M. Buffington[2]; Peter Goodwin, M.ASCE[3]; John G. King[4]; and William W. Emmett[5]

Abstract: Previous studies assessing the accuracy of bed-load transport equations have considered equation performance statistically based on paired observations of measured and predicted bed-load transport rates. However, transport measurements were typically taken during low flows, biasing the assessment of equation performance toward low discharges, and because equation performance can vary with discharge, it is unclear whether previous assessments of performance apply to higher, geomorphically significant flows (e.g., the bankfull or effective discharges). Nor is it clear whether these equations can predict the effective discharge, which depends on the accuracy of the bed-load transport equation across a range of flows. Prediction of the effective discharge is particularly important in stream restoration projects, as it is frequently used as an index value for scaling channel dimensions and for designing dynamically stable channels. In this study, we consider the geomorphic performance of five bed-load transport equations at 22 gravel-bed rivers in mountain basins of the western United States. Performance is assessed in terms of the accuracy with which the equations are able to predict the effective discharge and its bed-load transport rate. We find that the median error in predicting effective discharge is near zero for all equations, indicating that effective discharge predictions may not be particularly sensitive to one's choice of bed-load transport equation. However, the standard deviation of the prediction error differs between equations (ranging from 10% to 60%), as does their ability to predict the transport rate at the effective discharge (median errors of less than 1 to almost 2.5 orders of magnitude). A framework is presented for standardizing the transport equations to explain observed differences in performance and to explore sensitivity of effective discharge predictions.

DOI: 10.1061/(ASCE)0733-9429(2008)134:5(601)

CE Database subject headings: Stream improvement; Channel design; Geomorphology; Water discharge; Bed load.

Introduction

Bed-load transport is a fundamental physical process in alluvial rivers, building and maintaining a dynamically stable channel geometry that reflects both the quantity and timing of water and the volume and caliber of sediment delivered from the watershed (Leopold et al. 1964; Emmett and Wolman 2001). Accordingly, Leopold (1994) describes alluvial rivers as the architects of their own geometry (also see Parker 1978). Projects aimed at restoring the form and function of river ecosystems increasingly recognize the importance of channel geometry for dynamic equilibrium and the role of bed-load transport in forming and maintaining it (Goodwin 2004).

In these projects, the effective discharge is frequently used as an index value for scaling channel dimensions (Goodwin 2004). The effective discharge is defined as that which transports the greatest mass of sediment over time and is believed to control channel form in many alluvial rivers (Wolman and Miller 1960). The effective discharge is a fairly frequent event in sand- and gravel-bed rivers and is equivalent to the bankfull flow for channels in dynamic equilibrium (Andrews 1980; Carling 1988; Andrews and Nankervis 1995; Knighton 1998; Emmett and Wolman 2001), which in temperate climates tends to have a return period of 1–2 years (Wolman and Leopold 1957; Leopold et al. 1964; Williams 1978).

When site-specific transport data are not available, one is forced to predict the effective discharge from standard bed-load equations. Previous studies assessing the accuracy of bed-load transport equations have considered equation performance statistically based on paired observations of measured and predicted bed-load transport rates (e.g., Gomez and Church 1989; Yang and Huang 2001; Bravo-Espinosa et al. 2003; Barry et al. 2004). However, transport measurements were typically taken during low flows, biasing the assessment of equation performance toward low discharges (Fig. 1), and because equation performance can vary with discharge (Fig. 2 of Barry et al. 2004, 2007; Figs. 3–5 of Bravo-Espinosa et al. 2003; Fig. 5 of Habersack and

[1]Fluvial Geomorphologist, ENVIRON International Corp., 605 First Ave. Suite 300, Seattle, WA 98104 (corresponding author). E-mail: jbarry@environcorp.com

[2]Research Geomorphologist, Rocky Mountain Research Station, US Forest Service, Idaho Water Center, 322 East Front St., Suite 401, Boise, ID 83702.

[3]Professor, Center for Ecohydraulics Research, Dept. of Civil Engineering, Univ. of Idaho, Idaho Water Center, 322 East Front St., Suite 340, Boise, ID 83702.

[4]Retired Research Hydrologist, Rocky Mountain Research Station, US Forest Service, Idaho Water Center, 322 East Front St., Suite 401, Boise, ID 83702.

[5]Consulting Hydrologist, 5960 South Wolff Ct., Littleton, CO 80123.

Note. Discussion open until October 1, 2008. Separate discussions must be submitted for individual papers. To extend the closing date by one month, a written request must be filed with the ASCE Managing Editor. The manuscript for this paper was submitted for review and possible publication on May 17, 2006; approved on September 4, 2007. This paper is part of the ***Journal of Hydraulic Engineering***, Vol. 134, No. 5, May 1, 2008. ©ASCE, ISSN 0733-9429/2008/5-601–615/$25.00.

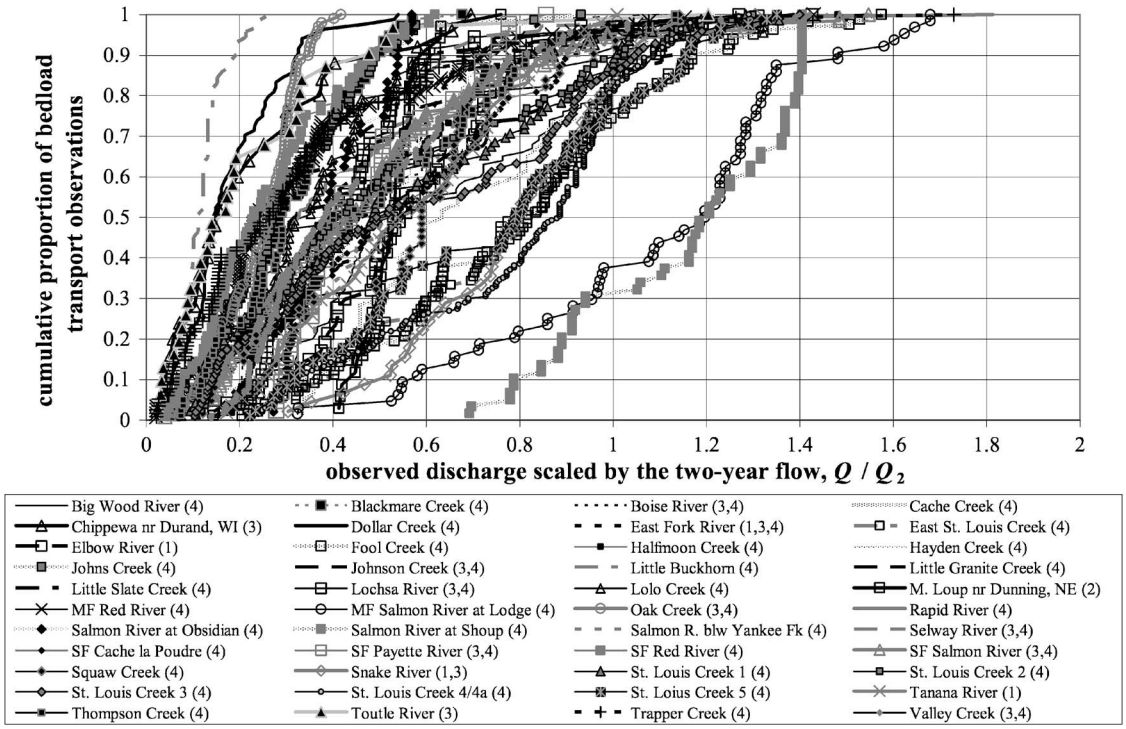

Fig. 1. Distributions of bed-load transport observations as function of discharge in gravel-bed rivers used in prior studies of equation performance. Numbers following each site name indicate studies using those data: (1) Gomez and Church (1989); (2) Yang and Huang (2001); (3) Bravo-Espinosa et al. (2003); and (4) Barry et al. (2004) . >80% of observations at each site typically occur at flows less than the two-year flood, Q_2, a bankfull-like flow (Whiting et al. 1999).

Laronne 2002), it is unclear whether previous assessments of performance apply to higher, geomorphically significant flows (e.g., the bankfull or effective discharges). Nor is it clear whether these equations can predict the effective discharge, which depends on the accuracy of the bed-load transport equation across a range of flows. In addition, previous assessments of equation performance focus on comparing observed versus predicted magnitudes of bed-load transport. However, accurate prediction of the effective discharge depends on how well a given transport equation predicts the rate of change in transport with discharge, rather than the absolute value of transport at a given discharge (Emmett and Wolman 2001; Goodwin 2004). Hence, the ability of bed-load transport equations to accurately predict the effective discharge and its transport rate remains to be tested.

A recent study by Goodwin (2004) developed analytical solutions for predicting effective discharge using generic forms of sediment transport equations and theoretical flow frequency distributions (normal, lognormal, and gamma). This study differs from his in that we examine the performance of specific, commonly used, bed-load transport equations, and we use observed flow frequency distributions because theoretical ones did not fit the data well.

Here, we consider the geomorphic performance of five different bed-load transport equations at 22 gravel-bed rivers in mountain basins of the western United States. Performance is assessed in terms of the accuracy with which the equations are able to predict the effective discharge and its bed-load transport rate. We also present a framework for standardizing the transport equations to explain observed differences in performance and to explore sensitivity of effective discharge predictions and their transport rates.

Effective Discharge

It is possible to directly compute the effective discharge at a site using the Wolman and Miller (1960) model if both the distribution of observed flows (from a nearby stream gauging station) and the sediment transport relationship (from direct measurements of bed-load transport and stream discharge) are known and representative of current conditions (Fig. 2). The product of discharge frequency (curve i) and bed-load transport rate (curve ii) over the range of discharges in the flow record describes the distribution of bed-load transport and the work done by the channel during that period (curve iii). The discharge where this product is maximized is termed the effective discharge (Wolman and Miller 1960) (Fig. 2). Controls on the prediction of effective discharge are examined below by parameterizing the Fig. 2 curves.

The bed-load transport rate (curve ii) can be represented by a power function of discharge (e.g., Gilbert 1914; Vanoni 1975; Emmett 1984; Smith et al. 1993; Whiting et al. 1999; Emmett and Wolman 2001; Bunte et al. 2004)

$$Q_b = \alpha Q^{\beta} \tag{1}$$

where Q_b=total bed-load transport rate (kg s^{-1}), Q=discharge (m^3 s^{-1}), and α and β=empirical values. The distribution of bed load transported over the period of record (curve iii) can be represented by the parameter Φ, which is the bed-load rating curve [Eq. (1)] multiplied by the frequency of occurrence of a given discharge, $f(Q)$, (curve i)

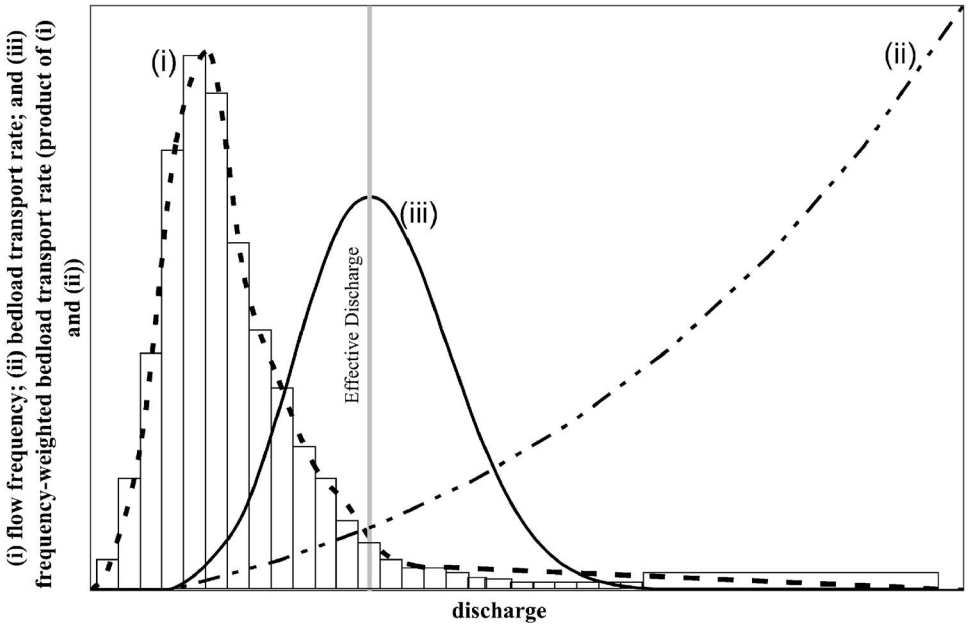

Fig. 2. Wolman and Miller (1960) model for magnitude and frequency of sediment transporting events. Curve (i) is flow frequency; curve (ii) is sediment transport rate as function of discharge; and curve (iii) is distribution of sediment transported during period of record (product of curves i and ii). Effective discharge is flow rate which transports most sediment over time, defined by maximum value of curve (iii). In this study, curve (i) is partitioned into arithmetic discharge bins (see Methods).

$$\Phi = \alpha Q^{\beta} f(Q) \tag{2}$$

The effective discharge (Q_e) occurs where Φ is at its maximum, such that $\partial\Phi/\partial Q = 0$ (Nash 1994; Goodwin 2004). Upon setting the partial derivative of Eq. (2) to zero, the coefficient of the bed-load rating curve, α, cancels out, with the effective discharge depending only on the exponent of the rating curve, β, and the characteristics of the flow distribution, $f(Q)$, (Nash 1994; Soar and Thorne 2001; Goodwin 2004). In addition to the overall shape of the flow frequency distribution, results can be particularly sensitive to adequate quantification of the frequency distribution in the range of flows close to the effective discharge (Goodwin 2004).

The sensitivity of effective discharge predictions to the rating-curve slope (β) is shown in Fig. 3. Larger values of β increase the predicted value of effective discharge for a given value of α [Fig. 3(a)]. In contrast, changes in α have no effect on the predicted value of effective discharge for a given value of β [Fig. 3(b)]; rather, as α increases, both the amount of transport at a given discharge and the bed-load yield over the period of record increase. The exponent of the bed-load rating curve is a function of supply-related channel armoring (transport capacity relative to sediment supply) (Barry et al. 2004, 2005). Poorly armored, fine-grained channels exhibit lower thresholds for bed-load transport and, thus, lower rating-curve exponents compared to well-armored, coarse-grained channels; consequently, poorly armored channels tend to have lower predicted values of effective discharge (Emmett and Wolman 2001; Goodwin 2004).

In this study, we are interested in assessing the ability of commonly used bed-load transport equations to accurately predict effective discharge and its transport rate. Fig. 3 provides a simple framwork for examining differences in performance of these equations in terms of α and β. However, use of this conceptual framework is complicated by the fact that most bed-load transport equations are not written in terms of simple rating curves [Eq. (1)], but rather are expressed in complex terms of excess shear stress or excess stream power (e.g., Appendix A of Barry et al. 2004). Therefore, in our analysis we predict total bed-load transport rates and consequent effective discharges in terms of the original formulations specified for each transport equation examined here. We then determine equivalent bed-load rating curves for transport rates predicted from each of these equations to examine their performance in terms of the Fig. 3 framework. Use of equivalent rating curves standardizes the diverse transport formulations to a common form that can be used in the Fig. 3 framework to explain observed differences in performance.

Study Sites and Methods

Bed-Load Transport Equations and Study Site Selection

The equations examined in this analysis are: (1) the Meyer-Peter and Müller (1948) equation (calculated by median subsurface grain size, d_{50ss}; (2) the Ackers and White (1973) equation as modified by Day (1980) (calculated by individual size class, d_i); (3) the Bagnold (1980) equation (calculated by the mode of the subsurface material, d_{mss}); (4) the Parker (1990) equation (calculated by d_i), with site-specific hiding functions (paragraph 89 of Barry et al. 2004); and (5) the Barry et al. (2004) equation as corrected in Barry et al. (2007) (summarized in Appendix I). In each equation, we used the characteristic grain size as originally specified by the author(s) to avoid introducing error or bias. The specific equations and our parameterization of them are presented elsewhere (Barry et al. 2004).

We examined the performance of these equations in mountain gravel-bed rivers of the western United States studied by Barry

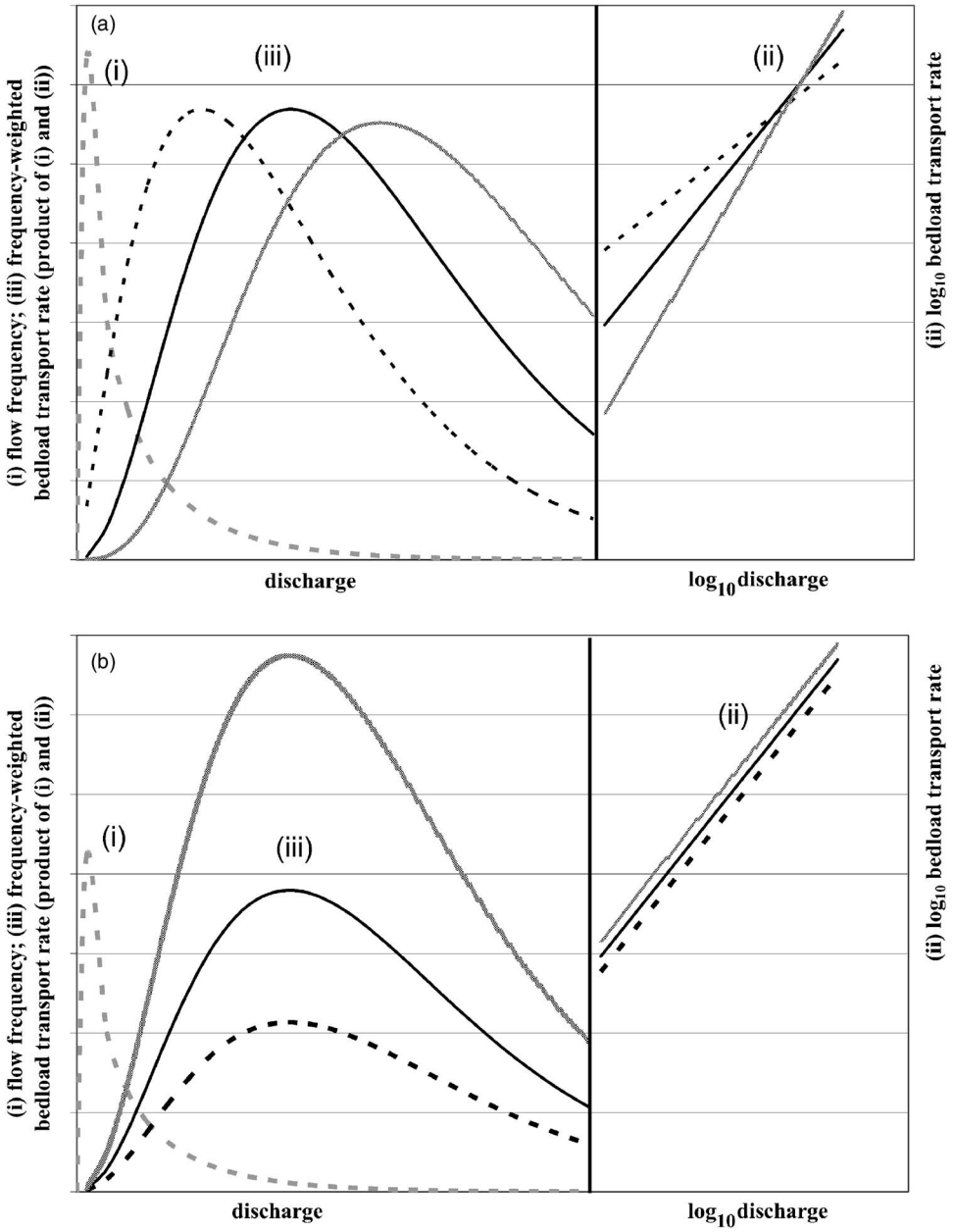

Fig. 3. Effect of: (a) changing the exponent of the bed-load rating curve, β; (b) changing the coefficient of the rating curve, α, on predictions of effective discharge and bed-load transport rate. Curve (i) is identical in both figures, α is constant in (a) and β is constant in (b).

et al. (2004). Local discharge records were combined with the above equations to predict the effective discharge and its associated transport rate at each site, and then compared to observed values determined from site-specific bed-load rating curves. To improve the accuracy of our analysis, we have only included those sites from Barry et al. (2004) where: (1) the observed record of daily mean discharge covers at least 10 years (Biedenharn et al. 2001); (2) the bed-load transport observations were made over a wide range of low to high flows; and (3) the observed bed-load transport data were adequately described by Eq. (1) [i.e., where the correlation coefficient (r^2) of the rating curve is greater than 0.70 and there is no obvious nonlinearity to the observed transport data in log space] (Nash 1994). Only 22 of the 41 sites examined by Barry et al. (2004) met these criteria and were used in the present analysis. The length of discharge observations at the study sites varies from 10 to 90 years, and the period of bed-load transport observations ranges from 1 to 13 years (Table 1).

Bed-load transport rates at these sites were observed across a range of flows from less than 10 to 180% of the 2-year flood (Q_2) (Fig. 4). However, the maximum discharge for which bed-load transport was measured at each site (Fig. 4, squares) is typically less than the maximum discharge of record (Fig. 4, diamonds). Consequently, in calculating the effective discharge, the observed bed-load rating curves were extrapolated to flows 2–80% larger (30% on average) than the largest flow for which bed-load observations were made. This extrapolation is unavoidable because few high-flow observations of transport are available due to unsafe field conditions during these events. Extrapolation error is likely reduced by our criteria for choosing sites with transport observa-

Table 1. Predicted and Observed Values of Effective Discharge

Site	Number of years in discharge/bed-load transport record (years)	Observed effective discharge ($m^3 s^{-1}$)	Predicted effective discharge ($m^3 s^{-1}$)				
			Meyer-Peter and Müller (1948)	Bagnold (1980)	Ackers and White (1973)	Parker (1990)	Barry et al. (2007)
Big Wood River	23/2	39.7	14.4	21.1	21.1	39.7	39.7
Boise River	90/4	175	115	18.0	127	175	139
Cache Creek	41/1	1.6	3.5	0.3	4.0	4.0	1.6
Dollar Creek	17/5	5.5	5.5	N.A.[a]	7.7	5.5	5.5
East Fork River	54/4	27.3	1.1	1.1	20.8	20.8	27.3
Halfmoon Creek	57/2	5.3	5.3	8.1	5.3	5.3	5.3
Hayden Creek	57/2	4.1	4.1	4.1	4.1	4.1	4.1
Johnson Creek	73/3	58.2	58.2	58.2	58.2	101	58.2
Little Granite Creek	11/13	6.52	5.4	5.4	9.4	13.3	6.52
Lochsa River	74/3	486	414	486	486	270	486
Lolo Creek	35/3	9.7	17.0	14.3	11.5	14.3	11.51
MF Red River	35/6	9.7	12.7	21.9	14.8	14.8	9.7
MF Salmon River at Lodge	10/1	363	160	363	228	363	363
Rapid River	88/7	21.2	17.1	3.0	25.2	25.2	21.2
Salmon River below Yankee Fork	67/2	166	120	97.6	166	178	166
Selway River	72/3	677	491	491	491	491	584
SF Cache la Poudre	23/2	9.0	9.0	11.6	9.0	9.0	9.0
SF Payette River	60/2	88.4	88.4	142	88.4	111	111
SF Salmon River	29/5	87.0	87.0	177	87.0	87.0	73
St. Louis Creek Site 1	69/5	4.9	3.5	3.5	4.9	4.9	4.9
St. Louis Creek Site 2	69/4	4.7	4.7	3.4	4.7	4.7	4.7
St. Louis Creek Site 3	69/4	4.7	4.7	4.7	4.7	4.7	4.7

[a]Bagnold (1980) equation predicted zero transport for all discharges in period of record.

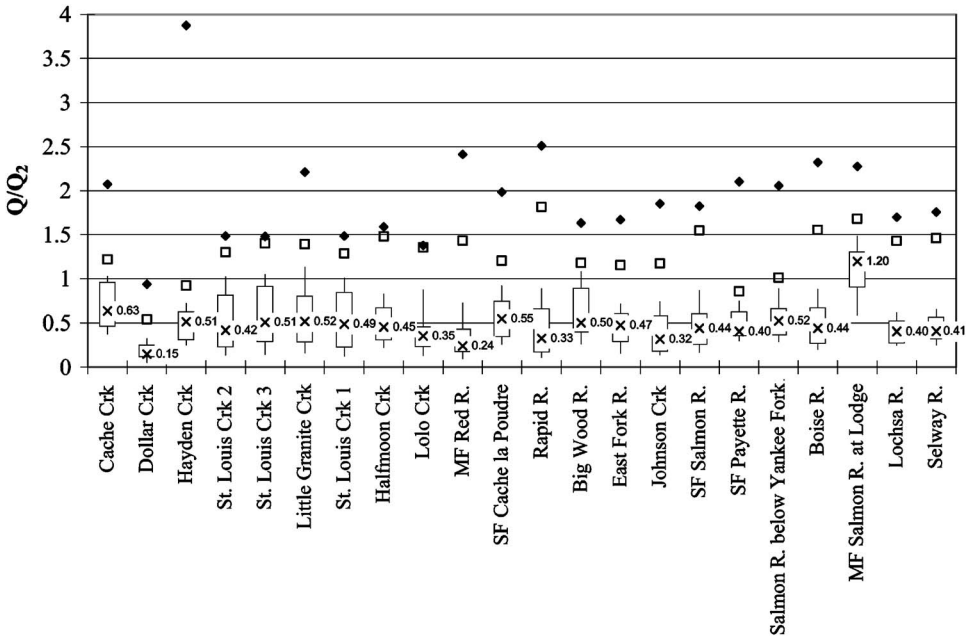

Fig. 4. Box plots of range of discharge, relative to Q_2, for which bed-load transport was measured at each site. Median values are specified by "X." Upper and lower ends of each box indicate interquartile range (25th and 75th percentiles). Extent of whiskers indicate 10th and 90th percentiles. Maximum discharges during period of record are shown by solid diamonds, while maximum discharges for bed-load transport observations are shown by open squares.

tions made over a broad range of discharges and with rating curves that have strong correlation coefficients ($r^2 > 0.7$).

Site Characteristics

The 22 sites are gravel-bed rivers located in mountain basins of Idaho, Colorado, and Wyoming, with hydrographs dominated by snowmelt runoff [see Table 1 for a list of the sites and Fig. 1 of Barry et al. (2004) for site locations]. They are single-thread channels with pool-riffle or plane-bed morphology (as defined by Montgomery and Buffington 1997). The stream banks of the study sites are typically composed of sand, gravel, and cobbles with occasional boulders and are well vegetated. Median surface grain sizes and channel slopes vary between 38 and 185 mm and 0.0021 and 0.0108, respectively. See Barry et al. (2004) for complete details of site characteristics and field methods.

Calculating Effective Discharge and Bed-Load Transport Rates

Flow frequency distributions at each of the 22 sites were discretized following the tabulation method of Biedenharn et al. (2001). The observed discharges were divided into 25, equal-width, arithmetic discharge bins, with a 26th bin for infrequent extreme events corresponding to the far right-hand tail of the flow distribution (Fig. 2, curve i). The representative discharge for each interval is taken as the arithmetic mean of each discharge class (Fig. 2).

Measured bed-load rating curves for each site were used to estimate the observed total bed-load transport rate for the arithmetic mean of each discharge bin (Q_{bi}). The product of the total bed-load transport rate and flow frequency within each discharge bin ($Q_{bi}.f(Q_i)$)=frequency-weighted transport for that bin (Φ_i). The effective discharge occurs where this product is maximized, and is taken as the arithmetic mean of that discharge bin. We assume that the transport rate for the average discharge of each bin is representative of the average transport rate across that bin, recognizing that this is an approximation that may not hold if bin sizes are too large, such that $\alpha\bar{Q}^{\beta}$ departs significantly from $\overline{\alpha Q^{\beta}}$.

Predicted values of effective discharge were determined in the same fashion, except that transport rates for each bin were predicted in terms of the original formulation of each transport equation, rather than in terms of bed-load rating curves. Predicted values of unit bed-load transport rate for each discharge bin (q_{bi}) were multiplied by flow width (w) to determine Q_{bi}, with w estimated from site-specific hydraulic geometry relationships. Shear stress and other necessary equation parameters for making these predictions were determined for each discharge following an approach similar to that used by Barry et al. (2004).

Other methods of estimating the effective discharge exist that do not require use of discharge bins, such as those presented by Goodwin (2004) and Emmett and Wolman (2001). In addition, Soar and Thorne (2001) discuss various types of binning methods (e.g., logarithmic discharge intervals). Discharge binning is probably the most common approach used by practioners to estimate effective discharge (e.g., Biedenharn et al. 2001; Soar and Thorne 2001), and so is used in this analysis. We have chosen to use arithmetic discharge intervals, rather than logarithmic ones, based on Soar and Thorne's (2001) finding that logarithmic binning tends to overpredict the effective discharge.

Results and Discussion

Estimating Effective Discharge

Fig. 5 shows box plots of the percent difference between predicted and observed values of effective discharge across the 22

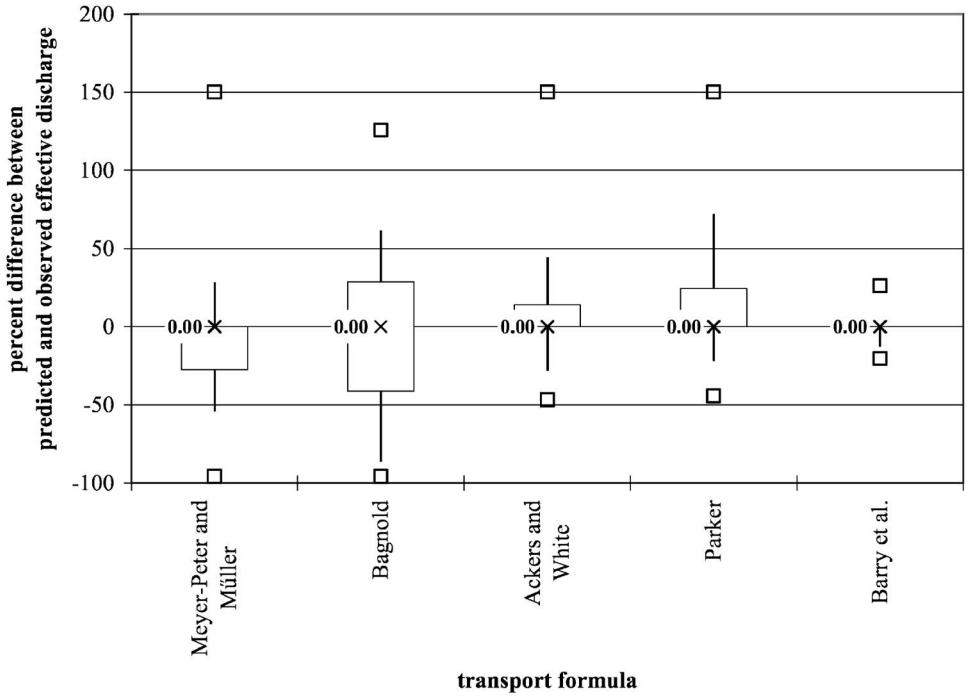

Fig. 5. Box plots of percent difference between predicted and observed effective discharge for each transport equation. Median values are specified by "X." Upper and lower ends of each box indicate interquartile range (25th and 75th percentiles). Extent of whiskers indicates 10th and 90th percentiles. Maximum outliers are shown by open squares.

sites using the five equations discussed above, with site-specific values reported in Table 1. The median prediction error is 0% for all equations (Fig. 5), indicating that effective discharge predictions may not depend on one's choice of bed-load transport equation. However, the standard deviation of the prediction error differs across the equations, ranging from 10% error for the Barry et al. (2007) equation to 60% for the Bagnold (1980) equation. The prediction errors for the Ackers and White (1973), Meyer-Peter and Müller (1948), and Parker (1990) equations have standard deviations of 40, 44, and 49%, respectively.

The performance of each equation was also assessed statistically in terms of the critical error, e^*, which is defined here as the percent difference between the predicted and observed effective discharge that one would have to tolerate to accept a given equation at a significance level of 0.05

$$e^* = \sqrt{\frac{196^2}{\chi^2}\sum_{i=1}^{n}\left(\frac{P_i - O_i}{O_i}\right)^2} \quad (3)$$

where P_i and O_i=respectively, predicted and observed values of effective discharge at a given site; n=number of observations, here equal to 22 (the number of sites); 196=value of the standard normal deviate corresponding to a two-tailed probability of 0.05 multiplied by 100; and χ^2=two-tailed chi-squared statistic with n degrees of freedom at a significance level of 0.05 (Freese 1960; Reynolds 1984).

Values of the critical error, e^*, range from a low of 14% for the Barry et al. (2007) equation to between 61 and 85% for the Ackers and White (1973) and Bagnold (1980) equations, respectively. Critical errors associated with the Meyer-Peter and Müller (1948) and Parker (1990) equations are 72 and 71%, respectively. These values of e^* differ from the median values of percent error shown in Fig. 5 because e^* is more representative of the overall prediction error.

We find that all of the equations examined here provide good estimates of the effective discharge (Fig. 5, median values), but performance can be quite variable across sites, with some equations performing better than others (Fig. 5, whisker ranges; and e^* analysis).

Sensitivity of Effective Discharge Prediction to Rating Curve Slope

As shown in Fig. 3, when using a simple bed-load rating curve to calculate the effective discharge for a given flow record, the predicted value is solely a function of β. As such, we would expect that transport equations with β values larger than the observed value will overpredict the effective discharge (i.e., differences greater than zero in Fig. 5). Of the equations examined here, only the Barry et al. (2007) equation is presented in the form of a rating curve with specified values of β. Nevertheless, equivalent rating-curve functions can be developed for the other transport equations if a two-part fit of β is used. A weighted average exponent ($\bar{\beta}$) of the two-part fit can then be compared to observed β values and equation performance can be evaluated within the framework presented in Fig. 3.

At each of the 22 sites, a weighted-average exponent, $\bar{\beta}$, was calculated for the Meyer-Peter and Müller (1948), Ackers and White (1973), Bagnold (1980), and Parker (1990) equations (Table 2). To do this, predicted bed-load transport rates were plotted as a function of discharge and fitted by Eq. (1) using a two-part fit of β: one fit to low flows and a second to higher flows. A weighted-average exponent ($\bar{\beta}$) was then calculated as the sum of the two fitted slopes weighted by the proportion of the total bed load transported in each discharge class. To check the accuracy of our weighting procedure, we compared the effective discharge predicted from the original formulation to that predicted from Eq. (1) with $\bar{\beta}$. The resultant average error is just under 5%, with a standard deviation of 12%.

Observed and predicted rating-curve exponents are shown in Table 2. Differences between predicted and observed values show that the Meyer-Peter and Müller (1948), Bagnold (1980), and Barry et al. (2007) equations typically underpredict the observed exponent by about 7–12% (Fig. 6, median values). In contrast, both the Ackers and White (1973) and Parker (1990) equations tend to overpredict the observed exponent by about 16–29% (Fig. 6, median values).

As hypothesized, we see a generally increasing linear relationship between errors in the rating-curve slope and errors in the prediction of the effective discharge (Fig. 7). However, many of the data are insensitive to errors in the rating-curve exponent and cluster along a line of zero error for prediction of effective discharge. This result is due to the characteristics of the underlying flow frequency distribution, which is explored further in Appendix II.

Bed-Load Transport Rate at Effective Discharge

At each of the 22 sites we compared the predicted bed-load transport rates from each equation, as originally formulated, to the observed transport rates at the observed effective discharge. We find that the performance of all five equations differs substantially in the accuracy with which they predict bed-load transport rate at the observed effective discharge (Fig. 8). Similar to previous studies (Gomez and Church 1989; Reid et al. 1996; Yang and Huang 2001; Habersack and Laronne 2002; Bravo-Espinosa et al. 2003; Barry et al. 2004), we find that most equations tend to overpredict. However, performance of a particular equation seems to be site specific. For example, Reid et al. (1996) show the Bagnold (1980) equation underpredicting at the Nahal Yatir in Israel, while Habersack and Laronne (2002) show it overpredicting at the Drau River in Austria, and Gomez and Church (1989) show it having roughly equal probability of over- or underpredicting at their study sites in North America. Similarly, we find that the Parker (1990) equation overpredicts bed-load transport at our study sites, while it was found to underpredict at study sites in both Austria (Habersack and Laronne 2002) and Israel (Reid et al. 1996), but to have equal probability of over- or underprediction at North American sites examined by Gomez and Church (1989, their Fig. 4). Consequently, equation performance varies across studies and sites. Furthermore, as discussed earlier, performance can vary with discharge. Our analysis focuses on performance at the effective discharge (a bankfull-like flow), while previous studies report average results across all observed flows, which are numerically biased toward a preponderance of low-flow observations. Hence, some of the discrepancy between studies may be due to the range of discharges used for assessing equation performance.

We also examined the critical error, e^*, in terms of log differences between predicted and observed transport rates (Freese 1960; Reynolds 1984)

Table 2. Observed α and β Values Compared to Those Determined from Fitting Eq. (1) to Predicted Transport Rates for Each Equation

	Observed		Meyer-Peter and Müller (1948)		Bagnold (1980)		Ackers and White (1973)		Parker (1990)		Barry et al. (2007)	
Site	α (95% confidence interval)	β (95% confidence interval)	$\bar{\alpha}$[a]	$\bar{\beta}$[a]	$\bar{\alpha}$[a]	$\bar{\beta}$[a]	$\bar{\alpha}$[a]	$\bar{\beta}$[a]	$\bar{\alpha}$[a]	$\bar{\beta}$[a]	$\bar{\alpha}$[a]	$\bar{\beta}$[a]
Big Wood River	4.86E−06 (2.3E−6–1.0E−5)	3.54 (3.26–3.82)	0.63[c]	1.83[c]	7.70E−3[c]	2.60[c]	9.10E−3[c]	2.91[c]	5.98E−6	4.32[c]	1.30E−5[c]	2.94[c]
Boise River	1.78E−06 (6.6E−7–4.8E−6)	2.86 (2.63–3.08)	3.09E−2[c]	2.12[c]	0.20[c]	1.34[c]	5.76E−4[c]	2.44[c]	7.06E−6[c]	3.19[c]	3.03E−6	2.57[c]
Cache Creek	6.00E−04 (4.9E−4–7.5E−4)	2.81 (2.40–3.22)	0.0517[c]	4.51[c]	27.98[c]	1.67[c]	3.40E−4[c]	4.80[c]	1.08E−5[c]	5.38[c]	5.80E−3[c]	1.67[c]
Dollar Creek	8.98E−04 (7.0E−4–1.2E−3)	2.40 (2.10–2.69)	0.195[c]	3.56[c]	N.A.[b]	N.A.[b]	1.01E−3	4.36[c]	3.50E−3[c]	2.66	5.41E−5[c]	2.84[c]
East Fork River	1.20E−03 (5.1E−4–2.9E−3)	2.19 (1.88–2.51)	0.394[c]	1.05[c]	0.102[c]	1.16[c]	4.94E−2[c]	1.54[c]	0.18[c]	1.55[c]	4.00E−4[c]	1.82[c]
Halfmoon Creek	1.66E−03 (1.3E−3–2.1E−3)	2.82 (2.63–3.01)	0.159[c]	3.65[c]	5.29E−4[c]	6.70[c]	6.50E−4[c]	3.75[c]	6.47E−4[c]	3.81[c]	8.00E−4[c]	2.11[c]
Hayden Creek	6.00E−03 (5.3E−3–6.7E−3)	2.36 (2.12–2.59)	2.85[c]	2.29	1.16[c]	2.00[c]	0.133[c]	2.82[c]	2.83E−3[c]	3.34[c]	4.40E−3[c]	2.30
Johnson Creek	2.84E−07 (1.2E−7–6.5E−7)	3.03 (2.79–3.27)	0.139[c]	1.86[c]	7.42E−3[c]	2.13[c]	1.21E−3[c]	2.41[c]	1.48E−7	4.68[c]	1.67E−6[c]	2.85
Little Granite Creek	3.08E−04 (2.2E−4–4.4E−4)	2.93 (2.69–3.16)	0.60[c]	2.30[c]	1.04[c]	1.73[c]	3.98E−3[c]	3.31[c]	4.29E−4	3.99[c]	6.93E−4[c]	2.10[c]
Lochsa River	3.04E−11 (2.1E−12–4.3E−10)	3.89 (3.40–4.38)	8.41E−5[c]	2.01[c]	4.33E−7[c]	4.52[c]	1.66E−9[c]	4.38	1.90E−4[c]	1.86[c]	5.6E−10[c]	3.59
Lolo Creek	2.53E−04 (1.6E−4–4.1E−4)	1.83 (1.57–2.10)	8.49E−6[c]	7.49[c]	3.44E−4	4.89[c]	2.47E−4	2.35[c]	2.58E−5[c]	5.00[c]	1.89E−4	2.23[c]
MF Red River	3.75E−04 (2.7E−4–5.2E−4)	2.38 (2.16–2.60)	3.46E−2[c]	3.88[c]	5.34E−7[c]	6.68[c]	1.14E−4[c]	3.89[c]	2.90E−3[c]	3.53[c]	4.56E−5[c]	3.04[c]
MF Salmon River at Lodge	2.10E−14 (4.7E−16–9.4E−13)	5.75 (5.07–6.43)	1.95E−2[c]	2.47[c]	1.95E−7[c]	5.06[c]	6.85E−6[c]	3.00[c]	8.03E−12[c]	6.32	2.78E−9[c]	3.72[c]
Rapid River	1.01E−04 (6.3E−5–1.6E−4)	2.32 (2.08–2.56)	0.279[c]	2.34	0.32[c]	1.50[c]	4.68E−4[c]	3.26[c]	6.20E−6[c]	4.45[c]	7.46E−5	2.69[c]
Salmon River below Yankee Fork	4.04E−09 (2.6E−10–6.2E−8)	3.85 (3.21–4.49)	3.70E−3[c]	2.76[c]	2.24E−4[c]	3.16[c]	2.17E−7[c]	3.58	5.34E−9	4.86[c]	6.32E−8	3.40
Selway River	7.05E−13 (5.1E−14–9.7E−12)	4.43 (3.97–4.88)	3.55E−3[c]	2.47[c]	3.46E−5[c]	2.91[c]	5.81E−7[c]	3.12[c]	7.65E−5[c]	2.42[c]	2.6E−10[c]	3.59[c]
SF Cache la Poudre	4.11E−04 (2.5E−4–6.6E−4)	2.62 (2.38–2.86)	0.148[c]	2.59	2.05E−3[c]	4.11[c]	2.68E−3[c]	2.91[c]	5.59E−2[c]	2.43	3.47E−5[c]	3.21[c]
SF Payette River	5.97E−07 (9.0E−8–4.0E−6)	3.46 (2.98–3.93)	1.89E−2[c]	2.44[c]	1.90E−7	5.44[c]	4.08E−6[c]	3.44	1.87E−6	3.74	2.66E−8[c]	3.77
SF Salmon River	1.88E−06 (5.7E−7–6.2E−6)	3.06 (2.73–3.38)	4.34E−5[c]	3.86[c]	3.2E−16[c]	9.19[c]	6.46E−8[c]	3.75[c]	7.84E−5[c]	2.72[c]	4.59E−5[c]	2.14[c]
St. Louis Creek Site 1	3.39E−03 (2.5E−3–4.6E−3)	2.15 (1.88–2.41)	2.18[c]	2.08	0.858[c]	2.06	1.60E−3	4.06[c]	2.34E−3	4.44[c]	1.20E−3[c]	2.13
St. Louis Creek Site 2	2.25E−03 (1.7E−3–3.0E−3)	2.22 (1.94–2.50)	0.953[c]	2.41	0.467[c]	2.10	1.08E−2[c]	3.46[c]	1.95E−2[c]	2.94[c]	6.05E−4[c]	2.64[c]
St. Louis Creek Site 3	1.13E−03 (8.3E−4–1.5E−3)	2.84 (2.58–3.11)	1.81[c]	2.19[c]	0.234[c]	2.75	1.59E−2[c]	3.43[c]	1.34E−4[c]	5.09[c]	3.07E−4	3.20[c]

[a] $\bar{\alpha}$ and $\bar{\beta}$ are weighted-average values (see *Estimating Effective Discharge*).

[b] Bagnold (1980) equation predicted zero transport for all discharges in period of record.

[c] Indicates predicted value outside 95% confidence interval.

$$e^* = \sqrt{\frac{1.96^2}{\chi^2}\sum_{i=1}^{n}[\log P_i - \log O_i]^2} \quad (4)$$

where P_i and O_i=respectively, predicted and observed bed-load transport rates for the observed effective discharge at a given site; n=number of observations (i.e., number of sites); 1.96=value of the standard normal deviate corresponding to a two-tailed probability of 0.05, and χ^2=two-tailed chi-squared statistic with n degrees of freedom at a significance level of 0.05. Only nonzero predictions are considered here, resulting in the exclusion of one predicted value (Table 1, Dollar Creek, Bagnold equation). Results show substantial differences in the amount of error one

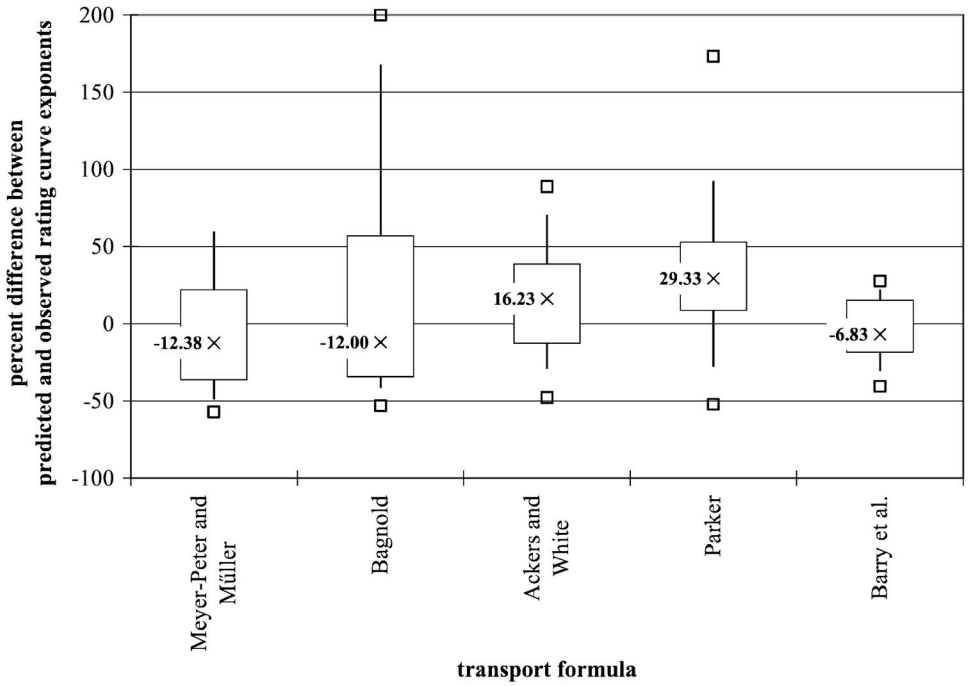

Fig. 6. Box plots of percent difference between predicted and observed bed-load rating curve exponents for each transport equation. Median values are specified by "X." Upper and lower ends of each box indicate interquartile range (25th and 75th percentiles). Extent of whiskers indicates 10th and 90th percentiles. Maximum outliers are shown by open squares.

would have to tolerate to accept a given prediction of the bed-load transport rate at the effective discharge. The Ackers and White (1973) and Parker (1990) equations have e^* values close to 1.75 orders of magnitude of error, whereas the Barry et al. (2007) equation has an e^* value less than 0.8 orders of magnitude of error (when discussing orders of magnitude, we use log units throughout). The e^* values for the Bagnold (1980) and the Meyer-Peter and Müller (1948) equations are equal to 2.1 and 3.2 orders of magnitude of error, respectively.

Accurate prediction of the total bed-load transport rate at a given discharge depends on the overall performance of the transport equation and may be sensitive to a variety of factors, including performance of transport threshold functions embedded within the equation, inclusion and accuracy of roughness correc-

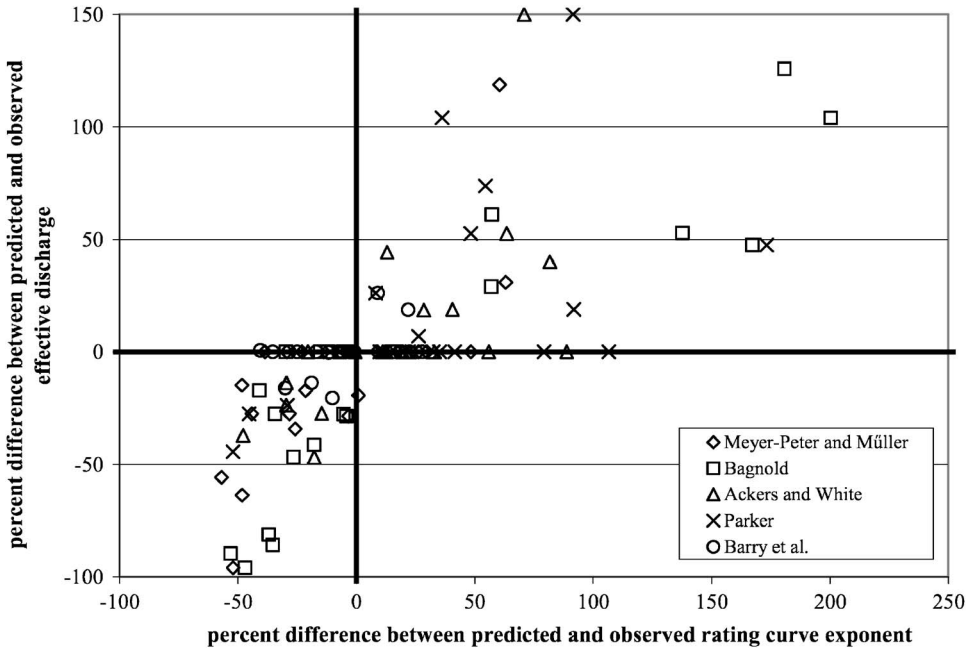

Fig. 7. Relationship between errors in predicted rating-curve exponent and errors in predicted effective discharge, both expressed as percent difference

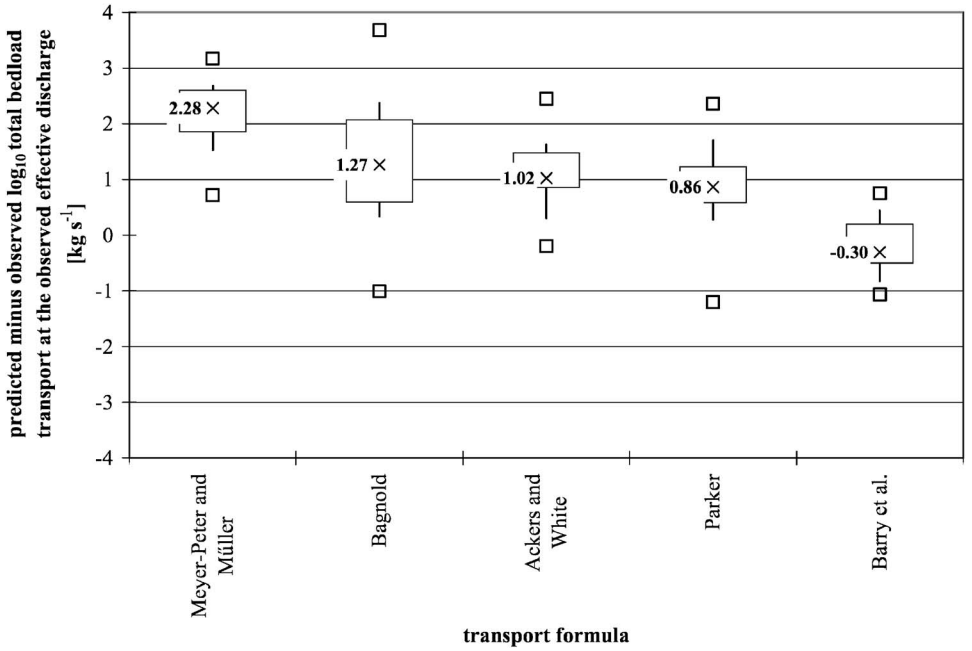

Fig. 8. Box plots of difference between predicted and observed log bed-load transport rates at observed effective discharge for each transport equation. Median values are specified by "X." Upper and lower ends of each box indicate interquartile range (25th and 75th percentiles). Extent of whiskers indicates 10th and 90th percentiles. Maximum outliers are shown by open squares.

tion parameters, and degree of equation calibration to site-specific conditions (Gomez and Church 1989; Barry et al. 2004). In terms of bed-load rating curves, this performance depends on the accuracy with which a given transport equation is able to reproduce the observed values of both α and β. We used the equivalent bed-load rating curves (both $\bar{\alpha}$ and $\bar{\beta}$) fit to the transport values predicted for each equation (Table 2) to standardize the various equations and to compare performance in terms of these rating curve values and the Fig. 3 framework. The Bagnold (1980) and Barry et al. (2007) equations both have predicted rating-curve slopes similar to the observed value [median errors in predicted β values of less than −0.056 and −0.032 orders of magnitude (or −12 and −7%), respectively; Fig. 6, Table 2]. However, the Bagnold (1980) equation overestimates α with a median prediction error of 2.4 orders of magnitude, whereas the Barry et al. (2007) equation has a median prediction error of less than −0.13 orders of magnitude (Table 2). As a result, the Bagnold (1980) equation overpredicts bed-load transport with a median error of almost 1.3 orders of magnitude, whereas the Barry et al. (2007) equation has a median prediction error of only −0.3 orders of magnitude (Fig. 8). We also find that the Ackers and White (1973) and Parker (1990) equations predict β with similar degrees of accuracy [median prediction errors of 0.07 and 0.11 orders of magnitude (or 16 and 29%), respectively; Fig. 6], however, the Parker (1990) equation predicts α more accurately than the Ackers and White (1973) equation (median prediction errors of 0.3 and almost 1.0 orders of magnitude, respectively). These differences in the relative accuracy of predicted α and β appear to be offsetting, in that both equations tend to overpredict bed-load transport at the effective discharge by similar amounts; almost an order of magnitude (Fig. 8).

Potential Error in Observed Transport Data

The observed bed-load rating curves at each site [Eq. (1)] are based on measured bed-load transport data from either a channel-spanning bed-load trap (East Fork River) or Helley–Smith samplers (all other sites). The channel-spanning trap captures essentially all of the bed-load in motion, whereas the Helley–Smith samples collect only a subset of the sediment in motion up to the width of the sampler orifice (3 or 6 in.). Because Helley–Smith samples are collected as a series of point measurements of limited duration along a cross section, while bed-load transport is a stochastic process in space and time, Helley–Smith measurements may not accurately sample the bed-load population, particularly the coarser sizes that move infrequently (Wilcock 2001). We assume that there is little error associated with the bed-load trap, but we are unable to quantify the error associated with the Helley–Smith measurements at our study sites (this would require having both bed-load trap and Helley–Smith samples at each site, which was not the case).

Habersack and Laronne (2002) did collect paired observations using a 6-in. Helley–Smith sampler and a pit trap and found that the Helley–Smith sampler gave comparable results. Similarly, Emmett (1980) found that the Helley–Smith sampler has near-perfect sediment trapping efficiency for particles between 0.5 and 16 mm in size. However, based on a number of simplifying assumptions, Hubbell and Stevens (1986) suggest a maximum probable error of 40% when using a Helley–Smith sampler to measure bed-load transport. Field studies by Bunte et al. (2004) indicate that Helley–Smith samples may overestimate transport rates by 3–4 orders of magnitude at lower flows (<50% bankfull), but with transport rates converging toward those measured by fixed traps at higher flows. Hence, the two methods should yield comparable estimates of bed-load transport at higher flows, which are the focus of this study. However, Bunte et al. (2004) show that bed-load rating curves for Helley–Smith samples tend to have lower slopes than those of traps. Because effective discharge calculations are sensitive to rating-curve slopes, differences in sampling methods may yield different estimates of the "observed"

effective discharge, and thus different results of equation performance when comparing observed versus predicted effective discharges.

Table 2 also reports the 95% confidence intervals for observed α and β values determined from Eq. (1), providing some sense of the uncertainty in the estimates of these values. The uncertainty in the observed rating-curve exponents varies from ± 7 to 17%, while the uncertainty of the coefficient varies from ± 2 to 14%. In contrast, between 70 and 90% of the predicted $\bar{\beta}$ values and 70–100% of the predicted $\bar{\alpha}$ values fall outside the 95% confidence intervals (Table 2 values marked with an asterisk).

The length of bed-load transport sampling records may introduce an additional source of uncertainty or error in the observed rating curves. For example, bed-load transport observations made over a single year will not include any year to year changes in sediment loads (Nordin 1980) and, depending upon when the samples were taken, may not incorporate the effect of annual hysteresis in bed load transport (Moog and Whiting 1998). At the 22 sites included in this analysis, bed-load transport observations were collected over a 1–13 year period, with two sites having only a single year of record, and six sites having only 2 years of record (Table 1). However, there is no systematic relationship between length of record and uncertainty in observed β values at our study sites (Table 2). Furthermore, because transport observations were collected over a range of flows on both the rising and falling limbs of the spring hydrographs in these snowmelt rivers, any effects of hysteresis are likely included.

Potential Bias with Barry et al. Equation

Thirteen of the 22 sites included in this analysis were part of the data from which the Barry et al. (2007) equation was derived. As a result, the portrayal of the Barry et al. (2007) equation as "best," compared to the other transport equations considered here, may be an artifact of having included a number of the calibration data sets in the current analysis. If we restrict the analysis to the nine sites not included in the development of the Barry et al. (2007) equation, the relative performance of the five bed-load transport equations shows only slight changes, with the exception of the Bagnold (1980) equation, whose median percent error in predicting the effective discharge decreases from 0 to −17%. However, equation-specific critical errors (e^*) for prediction of the effective discharge do change, with critical errors for both the Meyer-Peter and Müller (1948) and the Bagnold (1980) equations changing from 72 and 85% to 81 and 57%, respectively. Similarly, the e^* values associated with the Ackers and White (1973) and Parker (1990) equations change from 61 and 71% to 71 and 82%, respectively. The e^* value associated with the Barry et al. (2007) equation changes from 14 to 3%. Similar results are found when only the nine independent test sites are included in predicting the total transport at the effective discharge. Regardless of whether we use all 22 sites, or the subset of nine independent sites, the Barry et al. (2007) equation performs best for the rivers examined in this study. However, it remains to be seen how this equation performs in other gravel-bed rivers.

The superior performance of the Barry et al. (2007) equation also may be due, in part, to the fact that it is expressed as a rating-curve function, similar to that used to describe the observed transport data [Eq. (1)]. In particular, our estimates of the observed effective discharge and its transport rate may be influenced by the type of transport function fit to the observed data, which in turn could influence differences between observed and predicted values, and thus assessments of equation performance. In addition, the above nine sites are from physiographic and hydrologic environments similar to those used to develop the Barry et al. (2007) equation. Hence, they may not be geomorphically independent and further testing of our equation in different environments is warranted.

Conclusion

We find that prediction of the effective discharge is not particularly sensitive to the choice of bed-load transport equation (at least for those equations and study sites examined here) and that all equations predict the observed effective discharge reasonably well (with median errors of 0%, Fig. 5). However, equation performance differs both in terms of the range of effective discharge errors (Fig. 5) and in calculated values of critical error, e^*. Similarly, the accuracy of predicted bed-load transport rates at the effective discharge varies with equation selection, with most equations overpredicting transport rates by almost one to over two orders of magnitude (Fig. 8). Only the Barry et al. (2007) equation underpredicts bed-load transport (by −0.3 orders of magnitude) at the effective discharge.

Our finding that the prediction of effective discharge is insensitive to choice of bed-load transport equation corroborates the analytical results of Goodwin (2004), and suggests that even when the absolute value of sediment transport cannot be predicted accurately, it is possible to determine the channel forming or effective discharge. Consequently, the selection of an appropriate sediment transport equation depends on the intended application. For example, if the objective is modeling landscape evolution or the effective storage life of a dam, accurate prediction of the magnitude of sediment transport is critical, and therefore more care may be needed in selecting an appropriate transport equation. However, in channel restoration work, estimates of the requisite channel geometry and planform are sometimes obtained from empirical relations based on the effective discharge, rather than the magnitude of sediment transport at different flow conditions. For this case, our analysis suggests that any of the five equations examined here would provide a good estimate of the effective discharge on average, for the types of streams analyzed. The sensitivity of effective discharge predictions to variability of the flow frequency distribution is further discussed in Appendix II, where a relationship is derived that explains stability of effective discharge predictions as a function of discharge bin size, flow frequency, and β.

Although the effective discharge can be used as an index for restoration design, a suite of flows should be considered for successful restoration of physical processes and ecological function of rivers (Kondolf et al. 2001; Buffington and Parker 2005; Doyle et al. 2005; Smith and Prestegaard 2005; Wohl et al. 2005).

Acknowledgments

The writers are grateful once again to Sandra Ryan for providing data used in this study, and appreciate the insightful reviews provided by Rudy King, Charlie Luce, and two anonymous reviewers. This work was funded in part by the USDA Forest Service, Yankee Fork Ranger District (Grant No. 00-PA-11041303-071).

Appendix I. Barry et al. Equation

The Barry et al. (2004) equation as modified by Barry et al. (2007) is

$$q_b = \alpha(Q/Q_2)^{\beta} = 8.13 \cdot 10^{-7} A^{0.49} (Q/Q_2)^{(-2.45q^*+3.56)} \quad (5)$$

where q_b=total bed-load transport rate per unit width (kg m^{-1} s^{-1}); Q=discharge; Q_2=2-year flood, and α and β =empirical values that are further parameterized in terms of basin and channel characteristics to make the equation predictive. The coefficient α (kg m^{-1} s^{-1}) is parameterized as a power function of drainage area A (m^2), a surrogate for the magnitude of basin-specific bed-load supply, with the units of the drainage area coefficient ($8.13 \cdot 10^{-7}$) dependent on the site-specific regression between α and A (in our case, the units are kg m$^{-1.98}$ s^{-1}). The exponent β is parameterized as a linear function of q^* [a dimensionless index of channel armoring that is a function of transport capacity relative to bed-load supply (Dietrich et al. 1989)]. By parameterizing Eq. (5) in this fashion, we are proposing that the magnitude of bed-load transport depends, in part, on the basin-specific bed-load supply ($\alpha \propto A$) and that the slope of the transport function depends on the degree of channel armoring as influenced by transport capacity and bed-load supply ($\beta \propto q^*$) (see Barry et al. 2004 for further discussion).

Barry et al. (2004) define q^* as

$$q^* = \left(\frac{\tau_{Q_2} - \tau_{d_{50s}}}{\tau_{Q_2} - \tau_{d_{50ss}}} \right)^{1.5} \quad (6)$$

where τ_{Q_2}=total shear stress at Q_2 calculated from the depth-slope product (ρgDS, where ρ=fluid density; g=gravitational acceleration; D=flow depth at Q_2 calculated from site-specific hydraulic geometry relationships; and S=channel slope) and $\tau_{d_{50s}}$ and $\tau_{d_{50ss}}$=critical shear stresses necessary to mobilize the surface and subsurface median grain sizes, respectively, calculated from the Shields equation ($\tau_{d50} = \tau^*_{c50}(\rho_s - \rho) g d_{50}$) where the dimensionless critical Shields stress for mobilization of the median grain size (τ^*_{c50}) is set equal to 0.03, the lower limit for visually based determination of incipient motion in coarse-grained channels (Buffington and Montgomery 1997). See Barry et al. (2004) for further discussion of q^* and its influence on transport rates.

Appendix II. Sensitivity of Effective Discharge to Flow Frequency Distribution and Number of Discharge Bins

The sensitivity of effective discharge predictions to changes in β (Fig. 7) is largely determined by the variability of the flow frequency distribution surrounding the effective discharge bin. Moreover, the degree to which the effective discharge (Q_e) shifts to the left or right with changes in β depends on the flow frequency distribution that is used. When Q_e shifts to the left or right, it will move to the next largest Φ_i value of the work distribution Eq. (2). Work distributions derived from theoretical flow distributions (Goodwin 2004) are smoothly varying, such that the next largest Φ_i values are adjacent to the Q_e bin, causing Q_e to shift one bin to the left or right as β changes. In contrast, observed flow and work distributions are irregular (e.g., Goodwin 2004; his Figs. 3 and 4), with the next largest Φ_i value sometimes occurring several bins to the left or right of Q_e, causing Q_e to jump multiple bins with altered β. For example, at our sites we find that the effective discharge typically jumps four discharge bins with changes in β when observed flow frequency distributions are used (divided into 26 bins).

It is possible to develop an analytical solution to further explore the sensitivity of effective discharge estimates to changes or errors in the rating-curve slope, β. The total bed-load transport rate, Φ, is expressed as

$$\Phi_{L,e,R} = \alpha Q^{\beta}_{L,e,R} f(Q_{L,e,R}) \quad (7)$$

where the subscripts e, L, and R, respectively, indicate values for the effective discharge and those to the left and right of the effective discharge bin. The largest value of β before Q_e shifts to the right (i.e., to a larger discharge bin) occurs when $\Phi_e = \Phi_R$

$$\alpha Q_e^{\beta} f(Q_e) = \alpha Q_R^{\beta} f(Q_R) \quad (8)$$

Similarly, the smallest value of β before Q_e shifts to the left (i.e., to a smaller discharge bin) occurs when $\Phi_L = \Phi_e$

$$\alpha Q_L^{\beta} f(Q_L) = \alpha Q_e^{\beta} f(Q_e) \quad (9)$$

To allow for the possibility of Q_e shifting more than one discharge bin with changing β, Q_L and Q_R are generalized to Q_{nL} and Q_{nR}, where n=number of discharge intervals, or bins ΔQ, that Q_e moves, with $Q_{nL} = Q_e - n\Delta Q$, and $Q_{nR} = Q_e + n\Delta Q$. Combining Eqs. (8) and (9) and solving for β yields an expression describing the minimum and maximum β values before a change in the predicted effective discharge occurs (i.e., shifting Q_e to a neighboring discharge bin)

$$\frac{\log(f(Q_e)/f(Q_{nL}))}{\log(1 - n\Delta Q/Q_e)} \leqslant \beta \leqslant \frac{\log(f(Q_e)/f(Q_{nR}))}{\log(1 + n\Delta Q/Q_e)} \quad (10)$$

This equation describes the sensitivity, or robustness, of the predicted effective discharge to changes or errors in the rating-curve slope (β) for a given flow frequency distribution ($f(Q)$) and discharge interval (ΔQ). In particular, the minimum and maximum values which β can take before a change in Q_e occurs depend on the flow frequency of the effective discharge relative to that of its neighboring discharge bins ($f(Q_e)/f(Q_{nL})$ and $f(Q_e)/f(Q_{nR})$) and on the dimensionless size of the discharge bins ($n\Delta Q/Q_e$). Fig. 9 shows example plots of the upper and lower limits of β as a function of these parameters for n=1 (i.e., for shifting Q_e to an adjacent discharge bin). Absolute values of β increase with dimensionless bin size ($\Delta Q/Q_e$), but the predicted range of values that β can take before a shift in Q_e occurs depends on the flow frequency ratios (both in terms of their magnitude and asymmetry). For example, for a given value of $\Delta Q/Q_e$, the range in β values is smallest when $f(Q_L)/f(Q_e) = f(Q_e)/f(Q_R)$, and broader when $f(Q_L)/f(Q_e) < f(Q_e)/f(Q_R)$ (Fig. 9). As such, the variability of the flow frequency distribution about the effective discharge has a strong influence on the allowable range of β values before Q_e shifts to a neighboring discharge bin and, thus, the sensitivity of effective discharge predictions to changes or errors in β (Fig. 7). As expected, Fig. 9 also shows that larger flow frequency ratios ($f(Q_L)/f(Q_e)$, $f(Q_e)/f(Q_R)$) are required to move the effective discharge to an adjacent bin as values of β increase for a given dimensionless bin size ($\Delta Q/Q_e$). However, smaller dimensionless bin sizes require smaller relative changes in flow frequency about the effective discharge to shift Q_e to a neighboring bin. This suggests that results may be sensitive to the number of discharge bins used. We examined this issue for both observed and theoretical flow frequency distributions.

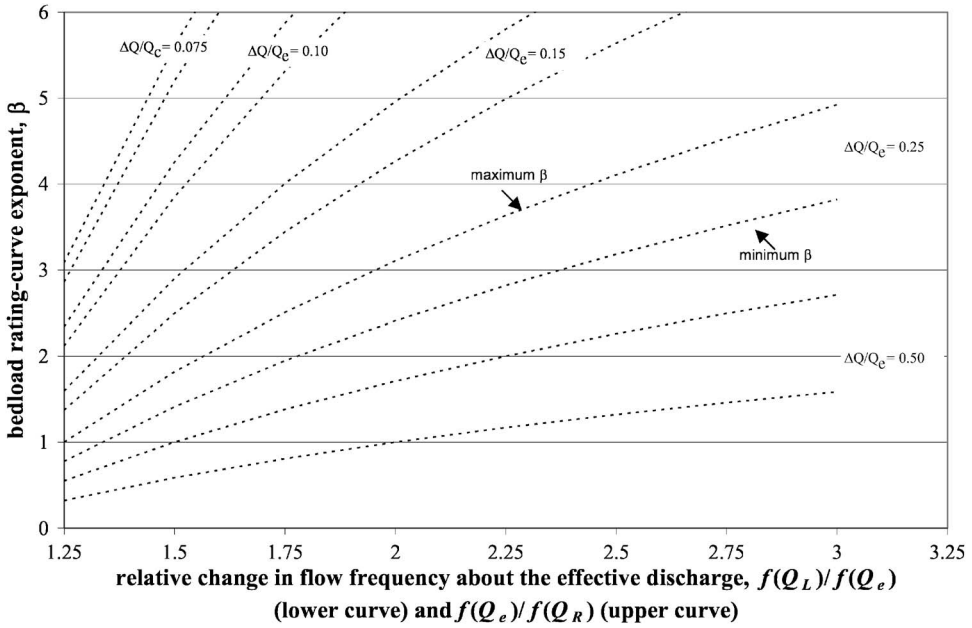

Fig. 9. Predicted ranges of bed-load rating-curve slope (minimum/maximum β) before effective discharge (Q_e) shifts to neighboring discharge bin, expressed as function of relative change in flow frequency about effective discharge ($f(Q_L)/f(Q_e)$ and $f(Q_e)/f(Q_R)$, where L and R indicate values for discharge bins to left and right of Q_e bin). For plotting convenience we inverted $f(Q_e)/f(Q_L)$ ratio in Eq. (10). Results are stratified by dimensionless bin size used for discretizing flow frequency distribution ($\Delta Q/Q_e$). Each pair of curves represents maximum and minimum β values determined from solution of left and right sides of Eq. (10), respectively, with $n=1$.

At our study sites, we find that the number of discharge bins typically has little effect on the effective discharge predictions (at least for the range of bin sizes examined, 6–50) (Fig. 10). However, results vary depending on the type of flow distribution used, with fitted theoretical distributions (normal, lognormal, or gamma) typically underpredicting the effective discharge. A gamma distribution results in effective discharge estimates that are most similar to the observed values. We also find that the range of allowable β [difference between maximum and minimum β values before a shift in Q_e occurs, Eq. (10)] depends on the number of discharge bins when theoretical frequency distributions are used, but is not a factor for observed flow distributions (Fig. 10). Furthermore, the observed flow distributions generally result in broader ranges of allowable β, explaining the insensitivity of Q_e predictions to errors in β (Fig. 7). These differences in behavior between observed and fitted theoretical flow distributions likely reflect differences in how the flow frequency ratios ($f(Q_L)/f(Q_e)$ or $f(Q_e)/f(Q_R)$) change with bin size and the irregular nature of observed flow frequency distributions compared to theoretical ones.

Notation

The following symbols are used in this paper:

A = drainage area (m^2);
D = flow depth (m);
d_i = grain size class (m);
d_{mss} = mode of subsurface material (m);
d_{50s} = median surface grain size (m);
d_{50ss} = median subsurface grain size (m);
e^* = critical error (either percentage, or log(kg s^{-1}));
$f(Q)$ = flow frequency;
$f(Q_e)$ = frequency of flow observations in effective discharge bin;
$f(Q_i)$ = flow frequency within ith discharge bin;
$f(Q_L)$ = frequency of flow observations in interval $Q_e - n\Delta Q$;
$f(Q_R)$ = frequency of flow observations in interval $Q_e + n\Delta Q$;
g = gravitational acceleration (m s^{-2});
n = number of observations, or number of discharge bins;
O_i = ith observed value;
P_i = ith predicted value;
Q = discharge (m^3 s^{-1});
Q_b = total bed-load transport rate (kg s^{-1});
Q_{bi} = total bed-load transport rate within discharge bin Q_i (kg s^{-1});
Q_e = effective discharge (m^3 s^{-1});
Q_i = discharge representing ith bin (m^3 s^{-1});
$Q_{L,R}$ = discharge in bin to left and right of effective discharge (m^3 s^{-1});
Q_2 = 2-year flood (m^3 s^{-1});
q^* = dimensionless index of channel armoring relative to sediment supply and transport capacity;
q_b = bed-load transport rate per unit width (kg m^{-1} s^{-1});
q_{bi} = bed-load transport rate per unit width within discharge bin Q_i (kg m^{-1} s^{-1});
S = channel slope (m m^{-1});
w = flow width (m);
α = coefficient in total bed-load transport rating curve;

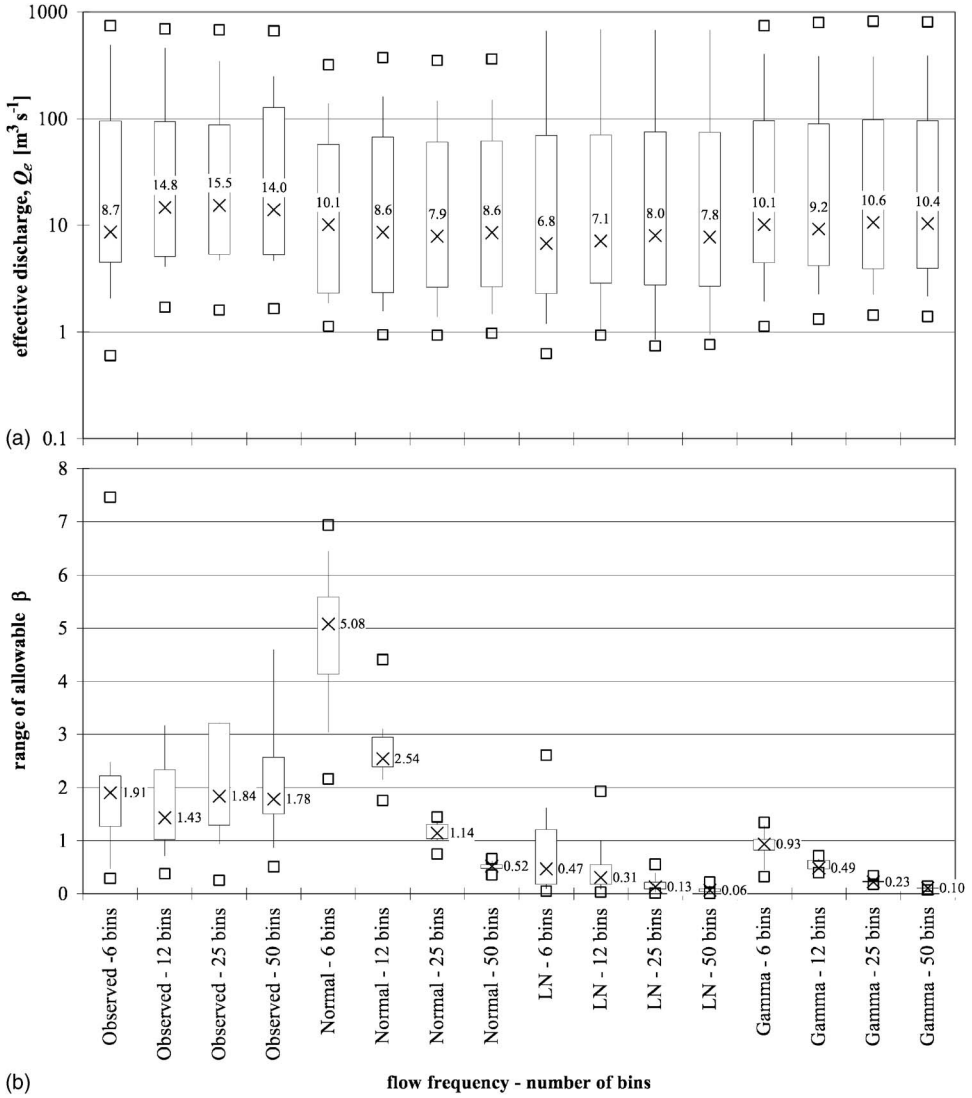

Fig. 10. Box plots of: (a) effective discharge; (b) range of allowable β [difference between maximum and minimum values of β before Q_e shifts discharge bins, Eq. (10)] at 22 field sites as function of number of discharge bins (6–50) and flow frequency type (observed, normal, log normal, gamma). Median values are specified by "X." Upper and lower ends of each box indicate interquartile range (25th and 75th percentiles). Extent of whiskers indicates 10th and 90th percentiles. Maximum outliers are shown by open squares.

$\bar{\alpha}$ = weighted average coefficient in bed-load transport rating curve;
β = exponent in total bed-load transport rating curve;
$\bar{\beta}$ = weighted average exponent in bed-load transport rating curve;
ΔQ = size of discharge bin ($m^3\ s^{-1}$);
ρ = fluid density ($kg\ m^{-2}$);
ρ_s = sediment density ($kg\ m^{-2}$);
τ^*_{c50} = dimensionless critical shear stress for median grain size;
$\tau_{d_{50s}}$ = critical shear stress of surface median grain size (Pa);
$\tau_{d_{50ss}}$ = critical shear stress of subsurface median grain size (Pa); and
τ_{Q_2} = total shear stress at Q_2 (Pa);
χ^2 = chi-square statistic;
Φ = frequency-weighted total bed-laod transport ($kg\ m^{-1}\ s^{-1}$);
Φ_i = frequency-weighted total bed-load transport within *i*th discharge bin ($kg\ m^{-1}\ s^{-1}$); and
$\Phi_{L,e,R}$ = frequency-weighted total bed-load transport for effective discharge bin and those to left and right of effective discharge bin ($kg\ m^{-1}\ s^{-1}$).

References

Ackers, P., and White, W. R. (1973). "Sediment transport: New approach and analysis." *J. Hydr. Div.*, 99, 2041–2060.

Andrews, E. (1980). "Effective and bank-full discharge in the Yampa River Basin, Colorado and Wyoming." *J. Hydrol.*, 46, 311–330.

Andrews, E. D., and Nankervis, J. M. (1995). "Effective discharge and the design of channel maintenance flows for gravel-bed rivers." *Natural and anthropogenic influences in fluvial geomorphology*, AGU Monograph Series 89, Washington, D.C., 151–164.

Bagnold, R. A. (1980). "An empirical correlation of bedload transport rates in flumes and natural rivers." *Proc. R. Soc. London, Ser. A*, 372, 453–473.

Barry, J. J., Buffington, J. M., and King, J. G. (2004). "A general power equation for predicting bedload transport rates in gravel bed rivers." *Water Resour. Res.*, 40, W104001.

Barry, J. J., Buffington, J. M., and King, J. G. (2005). "Reply to 'Comment by Claude Michel on A general power equation for predicting bedload transport rates in gravel bed rivers.'" *Water Resour. Res.*, 41, W07016.

Barry, J. J., Buffington, J. M., and King, J. G. (2007). "Correction to 'A general power equation for predicting bedload transport rates in gravel bed rivers.'" *Water Resour. Res.*, 43, W08702.

Biedenharn, D. S., Thorne, C. R., Soar, P. J., Hey, R. D., and Watson, C. C. (2001). "Effective discharge calculation guide." *Int. J. Sediment Res.*, 16(4), 445–459.

Bravo-Espinosa, M., Osterkamp, W. R., and Lopes, V. L. (2003). "Bedload transport in alluvial channels." *J. Hydraul. Eng.*, 129, 783–795.

Buffington, J. M., and Montgomery, D. R. (1997). "A systematic analysis of eight decades of incipient motion studies, with special reference to gravel-bedded rivers." *Water Resour. Res.*, 33, 1993–2029.

Buffington, J. M, and Parker, G. (2005). "Use of geomorphic regime diagrams in channel restoration." *EOS Trans. Am. Geophys. Union*, 86(52), Fall Meeting Supplement, Abstract H13E-1359.

Bunte, K., Abt., S. R., Potyondy, J. P., and Ryan, S. R. (2004). "Measurement of coarse gravel and cobble transport using portable bedload traps." *J. Hydraul. Eng.*, 130, 879–893.

Carling, P. (1988). "The concept of dominant discharge applied to two gravel-bed streams in relation to channel stability thresholds." *Earth Surf. Processes Landforms*, 13, 355–367.

Day, T. J. (1980). "A study of the transport of graded sediments." *Hydraulic Research Statistical Report No. IT190*, Wallingford, U.K., 10.

Dietrich, W. E., Kirchner, J., Ikeda, H., and Iseya, F. (1989). "Sediment supply and the development of the coarse surface layer in gravel-bedded rivers." *Nature (London)*, 340, 215–217.

Doyle, M. W., Stanley, E. H., Strayer, D. L., Jacobson, R. B., and Schmidt, J. C. (2005). "Effective discharge analysis of ecological processes in streams." *Water Resour. Res.*, 41, W11411.

Emmett, W. W. (1980). "A field calibration of the sediment-trapping characteristics of the Helley-Smith bedload sampler." *U.S. Geol. Surv. Prof. Pap. 1139*, Washington, D.C.

Emmett, W. W. (1984). "Measurement of bedload in rivers." *Erosion and sediment yield: Some methods of measurement and modelling*, R. F. Hadley, and D. E. Walling, eds., Geo Books, Norwich, U.K., 91–109.

Emmett, W. W., and Wolman, M. G. (2001). "Effective discharge and gravel-bed rivers." *Earth Surf. Processes Landforms*, 26, 1369–1380.

Freese, F. (1960). "Testing accuracy." *Forest Sci.*, 6, 139–145.

Gilbert, G. K. (1914). "The transportation of débris by running water." *U.S. Geol. Surv. Prof. Pap. 86*, Washington, D.C.

Gomez, B., and Church, M. (1989). "An assessment of bedload sediment transport formulae for gravel bed rivers." *Water Resour. Res.*, 25, 1161–1186.

Goodwin, P. (2004). "Analytical solutions for estimating effective discharge." *J. Hydraul. Eng.*, 130(8), 729–738.

Habersack, H. M., and Laronne, J. B. (2002). "Evaluation and improvement of bed load discharge formulas based on Helley-Smith sampling in an alpine gravel bed river." *J. Hydraul. Eng.*, 128(5), 484–498.

Hubbell, D. W., and Stevens, H. H. (1986). "Factors affecting accuracy of bedload sampling." *Proc., 4th Federal Interagency Sedimentation Conf., Subcomm. on Sedimentation*, Interagency Advisory Committee on Water Data, Las Vegas.

Knighton, D. (1998). *Fluvial forms and processes: A new perspective*, Oxford University Press, New York.

Kondolf, G. M., Smeltzer, M. W., and Railsback, S. (2001). "Design and performance of a channel reconstruction project in a costal California gravel-bed stream." *Environ. Manage. (N.Y.)*, 28, 761–776.

Leopold, L. B. (1994). *A view of the river*, Harvard University Press, Cambridge, Mass.

Leopold, L. B., Wolman, M. G., and Miller, J. P. (1964). *Fluvial processes in geomorphology*, Freeman, San Francisco.

Meyer-Peter, E., and Müller, R. (1948). "Formulas for bed-load transport." *Proc., 2nd Meeting of the Int. Association for Hydraulic Structures Research*, International Association Hydraulic Research, Delft, Netherlands, 39–64.

Montgomery, D. R., and Buffington, J. M. (1997). "Channel-reach morphology in mountain drainage basins." *Geol. Soc. Am. Bull.*, 109, 596–611.

Moog, D. B., and Whiting, P. J. (1998). "Annual hysteresis in bedload rating curves." *Water Resour. Res.*, 34, 2393–2399.

Nash, D. B. (1994). "Effective sediment-transporting discharge from magnitude-frequency analysis." *J. Geol.*, 102, 79–95.

Nordin, C. F. (1980). "Data collection and analysis." *Application of stochastic processes in sediment transport*, H. W. Shen, and H. Kikkawa, eds., Water Resources Publications, Littleton, Colo., 2-1–2-25.

Parker, G. (1978). "Self-formed straight rivers with equilibrium banks and mobile bed. Part 2. The gravel river." *J. Fluid Mech.*, 89, 127–146.

Parker, G. (1990). "Surface-based bedload transport relation for gravel rivers." *J. Hydraul. Res.*, 28, 417–436.

Reid, I., Powell, D. M., and Laronne, J. B. (1996). "Prediction of bedload transport by desert flash-floods." *J. Hydraul. Eng.*, 122, 170–173.

Reynolds, M. R. (1984). "Estimating error in model prediction." *Forest Sci.*, 30, 454–469.

Smith, R. D., Sidle, R. C., and Porter, P. E. (1993). "Effects on bedload transport of experimental removal of woody debris from a forest gravel-bed stream." *Earth Surf. Processes Landforms*, 18, 455–468.

Smith, S. M., and Prestegaard, K. L. (2005). "Hydraulic performance of a morphology-based stream channel design." *Water Resour. Res.*, 41, W11413.

Soar, P. J., and Thorne, C. R. (2001). "Channel restoration design for meandering rivers." *ERDC/CHL CR-01-1*, U.S. Army Corps of Engineers, Washington, D.C.

Vanoni, V. A. (1975). "Sediment discharge formulas," *Sedimentation engineering*, ASCE, New York, 190–229.

Whiting, P. J., Stamm, J. F., Moog, D. B., and Orndorff, R. L. (1999). "Sediment-transporting flows in headwater streams." *Geol. Soc. Am. Bull.*, 111, 450–466.

Wilcock, P. R. (2001). "Toward a practical method for estimating sediment-transport rates in gravel-bed rivers." *Earth Surf. Processes Landforms*, 26, 1395–1408.

Williams, G. P. (1978). "Bank-full discharge of rivers." *Water Resour. Res.*, 14, 1141–1154.

Wohl, E., et al. (2005). "River restoration." *Water Resour. Res.*, 41, W10301.

Wolman, M. G., and Leopold, L. B. (1957). "River floodplains: some observations on their formation." *U.S. Geol. Surv. Prof. Pap. 282-C*, 39–84.

Wolman, M. G., and Miller, J. P. (1960). "Magnitude and frequency of forces in geomorphic processes." *J. Geol.*, 68, 54–74.

Yang, C. T., and Huang, C. (2001). "Applicability of sediment transport formulas." *Int. J. Sediment Res.*, 16, 335–353.